Corrosion tests in liquid lithium-lead of multi-layer ceramic coatings

Erika Akahoshi[a], Moeki Matsunaga[a], Keisuke Kimura[a], Kazuki Nakamura[a], Martin Balden[b], Yoshimitsu Hishinuma[c], Takumi Chikada[a*]

[a]*Shizuoka University, Shizuoka, Japan*
[b]*Max-Planck-Institut für Plasmaphysik, Garching, Germany*
[c]*National Institute for Fusion Science, Gifu, Japan*

Tritium permeation through structural materials in fusion reactor blanket systems is a critical issue from the viewpoints of fuel loss and radiological safety. Ceramic coatings have been investigated to prevent tritium permeation; however, corrosion of the coatings by blanket materials, especially corrosive liquid tritium breeders such as lithium-lead is serious. In our previous study, the improvement of permeation reduction performance using an erbium oxide (Er_2O_3)-zirconium oxide (ZrO_2) two-layer coating was confirmed, but it did not show substantial corrosion resistance. In this study, various multi-layer coatings were fabricated by metal organic decomposition and then exposed to lithium-lead under static conditions to investigate precise corrosion behaviors of multi-layer coatings. After lithium-lead exposure for 1000 h at 600 ºC, the outermost Er_2O_3 layer almost disappeared, while the outermost ZrO_2 layer remained, indicating that ZrO_2 is more suitable as the outermost layer. However, many cracks and peelings were observed on the outermost ZrO_2 layer in the cases of the samples having four coating interfaces. The optimization of layer combination and the control of adhesion between the coatings are required to reduce the degradation of multi-layer coatings.

Keywords: Lithium-lead, Corrosion, Ceramic coating, Erbium oxide, Zirconium oxide

1. Introduction

Tritium permeation through structural materials in fusion reactor blanket systems is a critical issue from the viewpoints of fuel loss and radiological safety. One of the promising solutions is to fabricate a ceramic coating as a tritium permeation barrier on the blanket components. In our previous studies, precise deuterium permeation behaviors in the coatings have been clarified, and high permeation reduction performance was shown in ceramic coatings prepared by various methods [1]. In particular, metal organic decomposition (MOD) is one of the practical coating methods due to its possibility to fabricate on the components with complicated geometries. Moreover, the ceramic coatings such as erbium oxide (Er_2O_3) and zirconium oxide (ZrO_2) coatings fabricated by MOD showed high permeation reduction performance [2–4]. In liquid blanket concepts, however, corrosion of the coatings by liquid tritium breeders such as lithium-lead (Li-Pb) is an unavoidable problem. In our previous study, corrosion and peelings were confirmed after static Li-Pb exposure tests in single-layer coatings [5]. On the other hand, two-layer coatings consisting of Er_2O_3 and ZrO_2 were proposed as multi-functional coatings [6]. The two-layer coatings showed higher permeation reduction performance in comparison with the single-layer coatings, but they did not show an improvement of corrosion resistance. Although the improvement of corrosion resistance by further layering was possible, the effects of layer structure on corrosion resistance have not been clarified. In this study, multi-layer coatings with various layer structures were fabricated and then exposed to Li-Pb under static conditions for a further understanding of corrosion behaviors of multi-layer coatings.

2. Experimental details

2.1 Coating preparation

Reduced activation ferritic/martensitic steel F82H (Fe-8Cr-2W, F82H-BA07 heat) square plates with dimensions of 25 mm in length and 0.5 mm in thickness were used as substrates. The coating procedure is described in detail in Ref. [6]. First, the substrates were heat-treated in order to form a chromium oxide (Cr_2O_3) layer on the substrate and to prevent the peeling of MOD coatings [7]. The heat treatment was carried out for 10 min at 710 ºC in argon and hydrogen mixture flow with each flow rate of 50 standard cubic centimeters per minute (sccm). Thereafter, Er_2O_3 and ZrO_2 coatings were fabricated by MOD. The heat-treated F82H substrates were dipped into the coating precursors (Kojundo Chemical Laboratory Co., Ltd, Er-03® for Er_2O_3 and SYM-ZR04® for ZrO_2) and withdrawn at a constant speed of 1.0 mm s^{-1} using a dip coater.

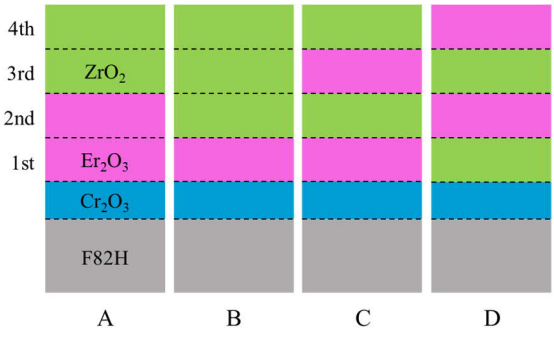

Fig. 1. Layer structures of multi-layer coatings.

*Corresponding author.
E-mail address: chikada.takumi@shizuoka.ac.jp (T. Chikada)

After withdrawal, the samples were dried for 6 min at 150 ºC and pre-heated for 2 min at 550 ºC in air using hot plates. The process of dipping, drying, and pre-heating was repeated twice, and then the coated samples were heat-treated for 30 min at 700 ºC in argon and hydrogen mixture flow with each flow rate of 50 sccm. The series of the process including the heat treatment was repeated four times to fabricate the multi-layer coatings. Fig. 1 summarizes layer structures of the multi-layer coatings. After a layer fabrication process, the thicknesses of the Er_2O_3 and ZrO_2 layers were approximately 50 nm and 150 nm, respectively. The coating thicknesses of each sample were approximately 400–500 nm.

2.2 Lithium-lead exposure test

Li-Pb exposure tests were performed under static conditions described in Ref. [8]. Li-Pb was synthesized from 99.9 % Li and 99.999 % Pb ingots purchased from Furuuchi Chemical Co. with the atomic ratio of 15.7:84.3 under argon atmosphere in a glove box. The synthesized Li-Pb contained impurities such as oxygen and carbon. In particular, oxygen is considered to have a significant effect on Li-Pb compatibility. In this study, Li-Pb was synthesized and the samples were soaked into Li-Pb under a low oxygen concentration environment (<1 vol% at atmospheric pressure) as described in our previous study [5]. From the oxygen concentration of the environment in the glove box and the ingots, we assume that Li-Pb used in this study contained 1000–10000 appm oxygen. The multi-layer coating samples cut into small specimens with the dimensions of 12 × 12 × 0.5 mm^3 were fixed by iron wires. After setting in an iron crucible, synthesized Li-Pb of 20–25 cc was poured into the crucible in argon atmosphere. After each crucible was encapsulated in a stainless steel container, the container was set in a muffle furnace. The Li-Pb exposure tests were conducted for 500–2000 h at 500–600 ºC. The Li-Pb exposure tests were conducted using one sample for each exposure temperature and duration. After exposure, the samples were picked up from liquid Li-Pb and shook out the adhered Li-Pb as much as possible. No cleaning process using ethanol and acetic acid was conducted in this study. Surface and cross-sectional observations of the samples were conducted by scanning electron microscopy (SEM) with energy dispersive X-ray spectroscopy (EDX) located at National Institute for Fusion Science, Japan and Max-Planck-Institut für Plasmaphysik, Germany. Cross-sectional SEM observation and EDX analysis for selected areas were conducted using a focused ion beam system. We observed the entire samples and analyze the trends. Additionally, we considered and discussed the trends in each sample based on the multiple results of the samples after the Li-Pb exposure tests.

3. Results

Fig. 2 shows surface SEM images of the samples before the Li-Pb exposure test. Smooth surfaces of the coatings were confirmed in as-prepared coatings. Table 1 summarizes the outlines of the results after the Li-Pb exposure tests. The deposition of a corrosion product was confirmed on all the sample surfaces after Li-Pb exposure. The EDX results showed that the corrosion product mainly consisted of carbon.

Table 1. Outline of result of Li-Pb exposure tests

	500 h, 500 ºC	500 h, 550 ºC	500 h, 600 ºC	1000 h, 600 ºC	2000 h, 600 ºC
Sample A	No degradation	No degradation	**Surface corrosion**	**Surface corrosion**	**Surface corrosion**
Sample B	**Interlamellar peeling**	No degradation	**Surface corrosion**	**Surface corrosion**	**Surface corrosion**
Sample C	**Interlamellar peelings**	No degradation	**Surface corrosion Peelings**	**Surface corrosion Cracks**	**Surface corrosion**
Sample D	**Surface corrosion Cracks**	**Surface corrosion Peelings**	**Surface corrosion Interlamellar peelings**	**Loss of layer Cracks**	**Loss of layers Peelings, Cracks**

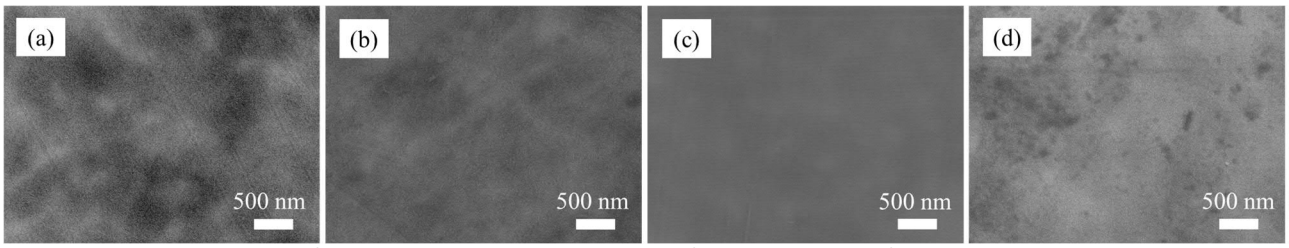

Fig. 2. Surface and cross-sectional SEM images of coating samples before Li-Pb exposure:
(a) Sample A, (b) Sample B, (c) Sample C, and (d) Sample D.

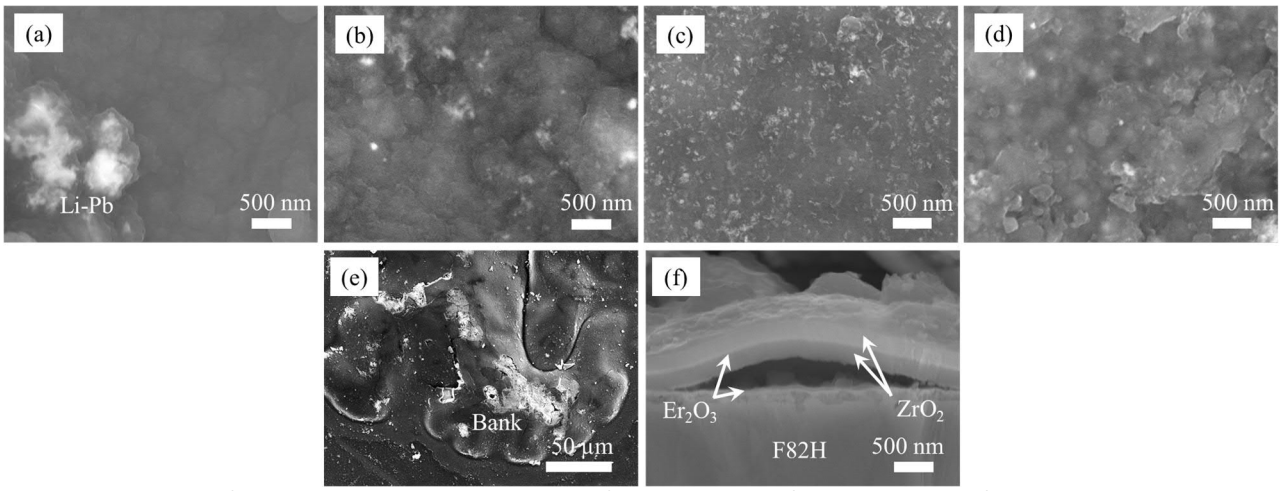

Fig. 3. Surface and cross-sectional SEM images of coating samples after Li-Pb exposure for 500 h at 500 ºC: (a) Sample A, (b) (e) Sample B, (c) (f) Sample C, and (d) Sample D.

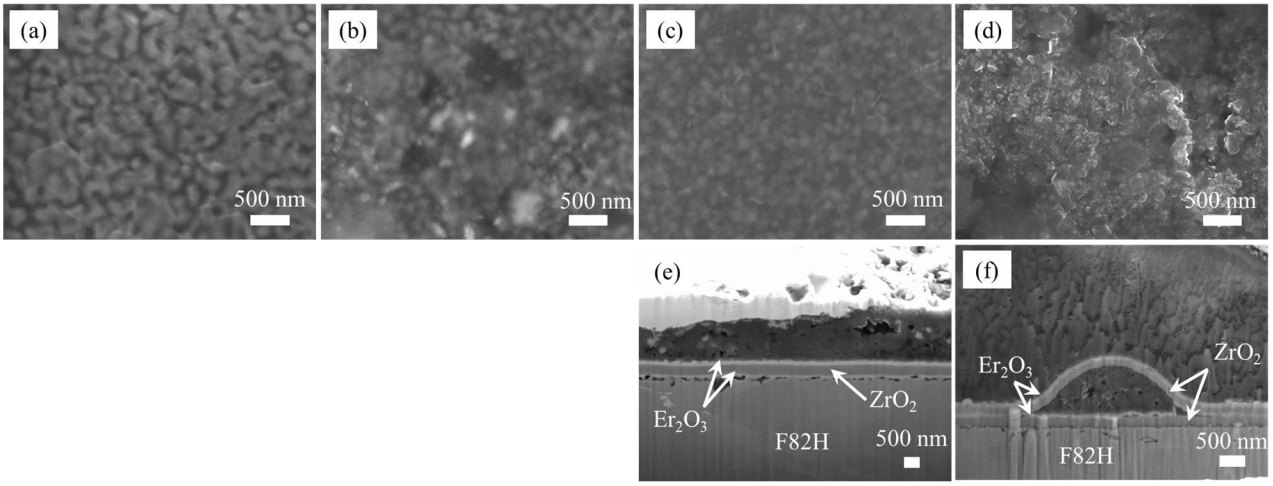

Fig. 4. Surface and cross-sectional SEM images of coating samples after Li-Pb exposure test for 500 h at 600 ºC: (a) Sample A, (b) Sample B, (c) (e) Sample C, and (d) (f) Sample D.

Fig. 3 shows surface and cross-sectional SEM images of the samples after Li-Pb exposure for 500 h at 500 ºC. Surfaces of Samples A–C that the outermost layer is ZrO_2 were smooth after exposure for 500 h at 500 ºC, which indicates negligibly little corrosion. On the other hand, Fig. 3(d) indicates the surface of the outermost Er_2O_3 layer became rough, suggesting that the corrosion occurred for Sample D. In addition, Fig. 3(e) shows a huge bank caused by an interlamellar peeling in Sample B. However, it was observed only in portion. The interlamellar peeling between the second Er_2O_3 layer and the third ZrO_2 layer was observed in Sample C, as shown in Fig. 3(f). Cracks and peelings were also confirmed around the area which the interlamellar peeling generated.

After the exposure test for 500 h at 550 ºC, no degradation was observed in Samples A–C, but peelings were observed in Sample D.

Surface and cross-sectional SEM images of the samples after Li-Pb exposure for 500 h at 600 ºC are shown in Fig. 4. After exposure, the outermost ZrO_2 layers of Samples A–C seemed to be corroded because the surfaces became rough, as shown in Fig. 4(a)–(c). In Sample D, the surface of the outermost Er_2O_3 layer became rougher than the samples after the Li-Pb exposure at 500 ºC and 550 ºC, as shown in Fig. 4(d), indicating that the corrosion depends on the test temperature. Peelings of the outermost ZrO_2 layer were confirmed in Sample C, and interlamellar peelings between the second Er_2O_3 layer and the third ZrO_2 layer were confirmed in Sample D, as shown in Fig. 4(e) and (f).

After the test for 1000 h at 600 ºC, corrosion further progressed in all the samples, compared with the tests for 500 h. In particular, in Sample D, the outermost Er_2O_3 layer was mostly lost by corrosion, and many cracks were observed in the third ZrO_2 layer. In Sample C, cracks were also confirmed on the outermost ZrO_2 layer. Surface SEM images of the samples after Li-Pb exposure for 2000 h at 600 ºC are shown in Fig. 5. Surface corrosion were confirmed in Samples A–C, while no degradation such as cracks and peelings was observed. Sample D lost one or two layers from the surface, and many cracks were observed in the remaining coatings. Moreover, the substrate was partly exposed on the surface.

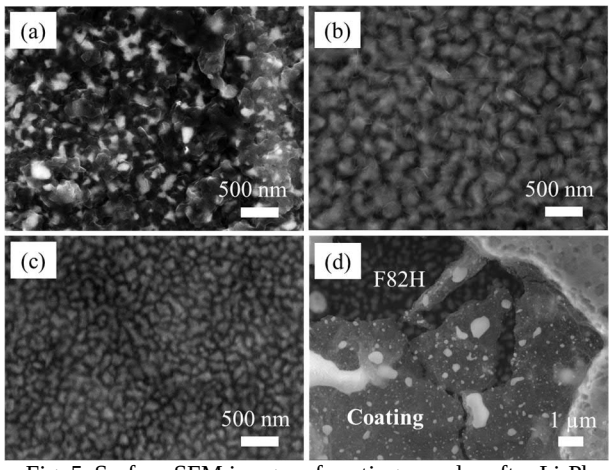

Fig. 5. Surface SEM images of coating samples after Li-Pb exposure test for 2000 h at 600 ºC: (a) Sample A, (b) Sample B, (c) Sample C, and (d) Sample D

4. Discussion

4. 1 Corrosion

We found that the corrosion behavior depended on coating material of the outermost layer. The corrosion of the outermost Er_2O_3 layer was confirmed by surface roughness after the Li-Pb exposure at 500–600 ºC. A corrosion process would be that Er_2O_3 was dissolved by a reaction with lithium and dissolved oxygen as proposed in the references [5,10]:

$$Er_2O_3 + 2Li + O[Li] \rightarrow 2LiErO_2 \quad (1)$$

This reaction might occur at lower temperature than 500 ºC from the result of Fig. 3(d) and be accelerated at higher temperatures. From the results of the exposure test for 1000 h and 2000 h at 600 ºC, the outermost Er_2O_3 layer was almost removed and it seemed to lose the function as a coating. On the other hand, the surface of the outermost ZrO_2 layer became rough only after the exposure tests at 600 ºC. Thus, ZrO_2 coatings would be corroded at higher temperature (≥ 600 ºC) via the following reaction:

$$ZrO_2 + 2Li + O[Li] \rightarrow Li_2ZrO_3 \quad (2)$$

The surfaces of all the samples after exposure for 2000 h were rougher than that for 500 and 1000 h. It was assumed that this reaction progressed with time.

The corrosion of the outermost Er_2O_3 layer was observed from 500°C, whereas that of ZrO_2 layer was observed only at 600°C. From these results, ZrO_2 is more suitable as an outermost layer than Er_2O_3.

4.2 Crack and peeling formation

The formation of cracks and peelings are mainly caused by changes in temperature during coating fabrication and/or the Li-Pb exposure tests because of a difference in the coefficient of thermal expansion (CTE) of the ceramic coatings. One of the causes of peeling is the invasion of Li-Pb and the carbon-based corrosion product through cracks and pores in the outermost layer.

In principle, Li-Pb corrosion progresses at high temperatures, but the stress on the coating due to the difference in CTE depends on the fabrication temperature. Since the coatings were heat-treated at 700 ºC, the compressive stress arose at the temperature lower than 700 ºC, and then the larger stress arose in the Li-Pb exposure tests at 500 ºC than 550 ºC, suggesting a cause of the interlamellar peeling of Samples B and C.

In Samples C and D, the coating degradation such as cracking and peeling was more serious than in Samples A and B based on the trends in all the test results. A common point between Samples A and B is that the outermost ZrO_2 layer was fabricated on the ZrO_2 layer, and these samples had two and three layers of ZrO_2 on the Er_2O_3 layer. In contrast, Sample C consisted of one outermost ZrO_2 layer on an inner Er_2O_3 layer, and Sample D consisted of one outermost Er_2O_3 layer on an inner ZrO_2 layer. When the coating repeated the fabrication process for four times with Er_2O_3 and ZrO_2 alternately, a stress caused by CTE mismatch would be so large that cracks easily generated during temperature change. On the other hand, the stress might be dispersed in the coating repeated the fabrication process with the same material, resulting in the prevention of crack formation. However, Sample B showed an interlamellar peeling at a single place after exposure for 500 h at 500 ºC. From these results, we consider that increasing the number of coating fabrication process is effective to mitigate the degradation of the coating, but the degradation might not be completely prevented.

Crack formation might have been suppressed by stress distribution due to increasing the number of coating fabrication process; therefore, less cracks might form in the outermost layer fabricated on the same material layer. Fig. 6 shows the possible mechanisms of the formation of crack and peeling. The sample that has less cracks in the outermost layer hardly causes peeling. Samples A and B indicated less cracks and peelings for these reasons. In contrast, the coating of Sample D formed cracks after the Li-Pb exposure test for 500 h at 500 ºC, and peelings were observed after the test at 550 ºC. We consider that only cracking might occur due to a CTE mismatch at 500 ºC, and the invasion of Li-Pb from the cracks cause peelings at 550 ºC.

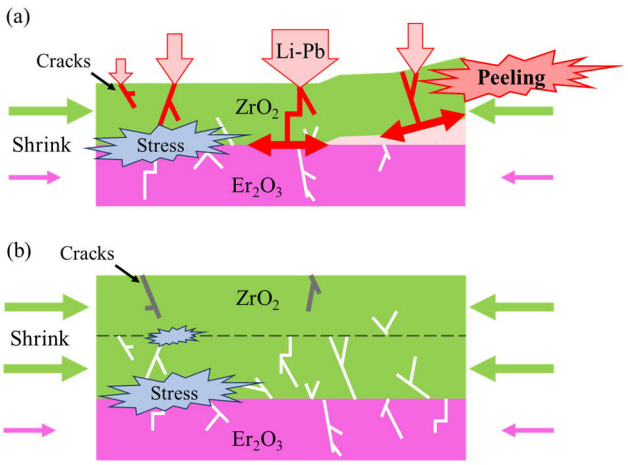

Fig. 6. Conceptual diagram of coating degradation in (a) ZrO_2 outermost layer on Er_2O_3 layer, (b) ZrO_2 outermost layer on Er_2O_3-ZrO_2 layer.

The interlamellar peelings in Sample D after Li-Pb exposure for 500 h at 600 ºC were observed the interface between the second Er_2O_3 layer and the third ZrO_2 layer. In Sample C, peelings of the outermost ZrO_2 layer on the Er_2O_3 layer as well as the interlamellar peeling were observed after Li-Pb exposure for 500 h at 600 ºC. From these results, the (F82H-)Er_2O_3-ZrO_2 interface would have lower integration than the ZrO_2-Er_2O_3 interface. One clear difference between the Er_2O_3 and ZrO_2 coatings is the coating thickness. In a report of the effect of the coating thickness on the stress and adhesion of the coatings with a thickness of ~200 nm, the coating thickness affects compressive stress and adhesive strength [10]. The thicknesses of the Er_2O_3 and ZrO_2 layers were approximately 50 and 150 nm, respectively. Since the ZrO_2 layer has a thickness three times as large as the Er_2O_3 layer, the interlamellar peeling might occur because of the difference in the adhesion of the layers. In addition, the fabrication process should be also considered to evaluate integrity of the multi-layer coatings in the further investigation.

5. Conclusion

Multi-layer coatings with various layer structures using Er_2O_3 and ZrO_2 were fabricated by MOD and then exposed to Li-Pb under static conditions. The observation after the Li-Pb exposure tests showed that the corrosion behavior varied with the test temperature and time as well as the layer structure. Corrosion proceeded in the outermost Er_2O_3 layer after all the exposure tests, and the most layer was lost after the exposure test for 1000 h at 600 ºC. On the other hand, corrosion progressed in the outermost ZrO_2 layer only after the exposure tests at 600 ºC. ZrO_2 would be more suitable as the outermost layer of multi-layer coatings than Er_2O_3. After the exposure test for 1000 h at 600 ºC, many cracks and peelings were observed in the coatings with three coating interfaces. In the coatings with the outermost ZrO_2 layer and one coating interface, less degradation was confirmed. The optimization of layer combination is important to reduce the degradation of multi-layer coatings. In addition, the thickness of the coating might be related to an integration between the coatings.

Acknowledgments

This work was supported by JSPS KAKENHI Grant Number 19H01873, the general collaboration research with National Institute for Fusion Science (NIFS18KEMF119), and Research Foundation for the Electrotechnology of Chubu Receipt Number E-01115.

References

[1] Ch. Linsmeier et al., Development of advanced high heat flux and plasma-facing materials, Nucl. Fusion 57 (092007) (2017) 60.

[2] T. Chikada et al., Surface behavior in deuterium permeation through erbium oxide coatings, Nucl. Fusion 51 (063023) (2011) 5.

[3] T. Chikada et al., Microstructure control and deuterium permeability of erbium oxide coating on ferritic/martensitic steels by metal-organic decomposition, Fusion Eng. Des. 85 (2010) 1537–1541.

[4] T. Chikada et al., Crystallization and deuterium permeation behaviors of yttrium oxide coating prepared by metal organic decomposition, Nucl. Mater. Energy 9 (2016) 529–534.

[5] M. Matsunaga et al., Lithium-lead corrosion behavior of erbium oxide, yttrium oxide and zirconium oxide coatings fabricated by metal organic decomposition, J. Nucl. Mater. 511 (2018) 534–543.

[6] J. Mochizuki et al., Preparation and characterization of Er_2O_3-ZrO_2 multi-layer coating for tritium permeation barrier by metal organic decomposition, Fusion Eng. Des. 136 (2018) 219-222.

[7] T. Tanaka et al., Control of substrate oxidation in MOD ceramic coating on low-activation ferritic steel with reduced-pressure atmosphere, J. Nucl. Mater. 455 (2014) 630–634.

[8] T. Chikada et al., Fabrication technology development and characterization of tritium permeation barriers by a liquid phase method, Fusion Eng. Des. 136 (2018) 215–218.

[9] M. Nagura et al., $LiErO_2$ formation on Er_2O_3 in static and natural convention lithium, Fusion Eng. Des. 84 (2009) 1384–1387.

[10] D. Sheeja et al., Effect of film thickness on the stress and adhesion of diamond-like carbon coatings, Diamond Related Mater. 11 (2002) 1643–1647.